Acta Biochim Biophys Sin, 2015, 47(6), 451–458
doi: 10.1093/abbs/gmv034
Advance Access Publication Date: 5 May 2015
Original Article

Original Article

Heat shock protein 90 mediates the apoptosis and autophage in nicotinic-mycoepoxydiene-treated HeLa cells

Yifei Sun, Shuyan Xiao, Junjie Chen, Miaomiao Wang, Zhonghui Zheng, Siyang Song, and Lianru Zhang*

Key Laboratory for Cell Stress, School of Life Sciences, Xiamen University, Xiamen 361102, China

*Correspondence address. Tel/Fax: +86-592-2181722; E-mail: ru898@xmu.edu.cn

Received 14 November 2014; Accepted 14 January 2015

Abstract

Heat shock protein 90 (Hsp90) is a fascinating target for cancer therapy due to its significant role in the crossroad of multiple signaling pathways associated with cell proliferation and regulation. Hsp90 inhibitors have the potential to be developed into anti-cancer drugs. Here, we identified nicotinic-mycoepoxydiene (NMD), a structurally novel compound as Hsp90 inhibitor to perform the anti-tumor activity. The compound selectively bound to the Hsp90 N-terminal domain, and degraded the Hsp90 client protein Akt. The degradation of Akt detained Bad in non-phosphorylation form. NMD-associated apoptosis was characterized by the formation of fragmented nuclei, poly(ADP-ribose) polymerase cleavage, cytochrome *c* release, caspase-3 activation, and the increased proportion of sub-G1 phase cells. Interestingly, the apoptosis was accompanied with autophagy, by exhibiting the increased expression of LC-3 and the decrease of lysosome pH value. Our findings provide a novel cellular mechanism by which Hsp90 inhibitor adjusts cell apoptosis and autophagy *in vitro*, suggesting that NMD not only has a potential to be developed into a novel anti-tumor pharmaceutical, but also exhibits a new mechanism in regulating cancer cell apoptosis and autophagy via Hsp90 inhibition.

Key words: heat shock protein 90 (Hsp90), inhibitor, apoptosis, autophagy, HeLa cell

Introduction

Heat shock protein 90 (Hsp90) is a novel target for anti-cancer agents because of its unique ability to be selectively associated with signaling molecules with abnormal expression level in cancer cells that implicated in the aberrant survival of cancer cells [1,2]. Hsp90 is required for stabilizing many important proteins. Its inhibitors can simultaneously inhibit multiple signaling pathways that cancer cells depend on for their growth and proliferation [3]. So the selective inhibition of Hsp90 consequently inhibits the aberrant survival signaling pathway, which can induce apoptosis in cancer. The discovery of natural products that display anti-tumor activity by inhibiting Hsp90 function brought about a promising new class of pharmaceuticals [4]. Hsp90 inhibitors have already shown promising anti-tumor activity in preclinical model systems [5–8]. It has been shown that the characterization of new Hsp90 inhibitors has the potential to lead to the development of potent anti-cancer drugs and small molecular probes [9].

Mycoepoxydiene (MED) was initially isolated from the marine fungus *Diaporthe phaseolorum* HLY2 strain and was identified as a lead compound with anti-cancer activity [10]. It has been suggested that the main molecular target of MED is Hsp90, but the inhibitory activity of MED toward Hsp90 is lower than those well-characterized Hsp90 inhibitors such as geldanamycin (GA) [11–13]. Therefore, a derivative of MED with a nicotinic moiety, nicotinic-mycoepoxydiene (NMD) was rationally designed and synthesized with improved potency compared with that of MED [14].

Our preliminary experiments found that the activity of NMD toward Hsp90 degraded its client protein, e.g. Akt, associated with HeLa cell apoptosis and autophagy. The autophagosomes were

involved in mitochondrial clearance cascades in NMD-treated HeLa cells. There are many reports that highlight the Hsp90 inhibitors induced cancer cell apoptosis, but few reports have been focusing on autophagy-associated apoptosis.

In this study, we provided insight into NMD's anti-cancer mechanism and revealed that NMD could serve as a potent therapeutic agent against cancer. More importantly, NMD could be used as a probe to uncover the mechanism of cellular autophagy and apoptosis. Our results provided the clues of NMD inhibition of cancer cell growth via degrading the Hsp90 client protein. The degradation of Akt resulted in the decreased level of Bad phosphorylation and initiated NMD-induced mitochondria apoptosis and autophagy in HeLa cells.

Materials and Methods

Materials

NMD was synthesized according to the previously described method [15]. The following reagents were purchased from Sigma-Aldrich (St Louis, USA): propidium iodide (PI), 4′,6-diamidino-2-phenylindole (DAPI), GA, carbobenzoxy-valyl-alanyl-aspartyl-[O-methyl]-fluoromethylketone (z-VAD-fmk), 5-(and-6)-chloromethyl-2′-7′-dichlorodihydrofluorescein diacetate, acetyl ester (CM-H2DCFDA), dithiothreitol, 3-(4,5-dimethylthiazol-2-yl)-2,5-diphenyltetrazolium bromide (MTT), 5,5,6,6′-tetrachloro-1,1,3,3′-tetraethyl-imidacarbocyanineiodide (JC-1), Pyrrolidinedithiocarbamic acid, ammonium salt, monodansylcadaverin (MDC), and RNaseA.

Cell culture

Human liver cell line (LO2), cervical carcinoma cell line (HeLa), and other tumor cell lines (AML-21, MD-MBA-231, U2Os, and HL-60) were obtained from the cell line bank at the School of Life Sciences at Xiamen University (Xiamen, China). The cells were maintained in Dulbecco's modified Eagle's medium (DMEM; Gibco, Carlsbad, USA) supplemented with 10% new fetal calf serum (Gibco) at 37°C in a 5% CO_2-enriched and humidified environment.

Cell cycle analysis

HeLa cells were cultured in DMEM supplemented with 10% fetal bovine serum in a 37°C incubator humidified with 5% CO_2. The cells were trypsinized at 24 h post-NMD treatment, then collected by centrifugation, washed once with phosphate-buffered saline (PBS), and re-suspended in PBS containing 5 μg/ml PI. The level of PI incorporation was quantitated by a FACScan flow cytometer (Beckman Coulter, Pasadena, USA). Apoptotic cells were defined as those arrested at the sub-G1 phase.

Cell survival rate analysis

The cells were treated with NMD for different durations. After that, the cells were harvested and fixed in 70% cold ethanol, followed by centrifugation and washing. The fixed cells were stained with PI (50 μg/ml) and analyzed by a FACScan flow cytometer. With proper gating of major population of cells by adjusting Forward Scatter, Side Scatter, and Fluorescence 1 (FL1) level, the signals produced by cells located in low FL1 signal region were identified as living cells. The proportion of living cells in total cells was calculated as survival rate.

Western blot analysis

Nuclear and cytoplasmic proteins were extracted with Extraction Kits (Beyotime, Beijing, China). The cultured cells were washed with PBS and lysed with lysis buffer (50 mM Tris–HCl, 150 mM NaCl, 0.5% Triton X-100, and 1 mM EDTA; pH 7.4) supplemented with a protease inhibitor mixture. The samples containing the same amount of total proteins were resolved on sodium dodecyl sulfate–polyacrylamide denaturing gels, transferred to nitrocellulose membranes, and probed with the specific antibodies: anti-p-Bad (Ser136) (1:1000; Cell Signaling, Beverly, USA), anti-p-Akt (Ser473) (1:1000; Cell Signaling), anti-Akt (1:1000; Cell Signaling), anti-Bcl-2 (1:1000; Cell Signaling), anti-Bad (1:1000; Cell Signaling), anti- poly(ADP-ribose) polymerase (PARP) (1:1000; Cell Signaling), and anti-LC-3I/II (1:1000; Santa Cruz, Santa Cruz, USA). Horseradish peroxidase-conjugated Immuno-pure goat anti-mouse or anti-rabbit antibodies were used as secondary antibodies (Pierce, Rockford, USA).

Mitochondrial membrane potential measurements

HeLa cells were treated with NMD for 24 h. The cell suspension (0.5 ml) was then transferred into a sterile centrifuge tube and centrifuged at 400 *g* for 5 min. The supernatant was then removed, and the cells were suspended in 0.5 μM JC-1 reagent, followed by incubation at 37°C for 15 min. Relative fluorescence intensities were monitored by flow cytometry. And both the red fluorescence (excitation at 550 nm and emission at 600 nm) and green fluorescence (excitation at 485 nm and emission at 535 nm) were measured with a fluorescence microscope (Zeiss, Oberkochen, Germany). In this assay, the ratios of red fluorescence to green fluorescence decreased in the dead cells and in the cells undergoing apoptosis when compared with that in the healthy cells [16,17].

Detection of apoptosis by immunofluorescent staining

To measure cytochrome *c* release, HeLa cells were seeded onto glass coverslips that were pre-coated with 0.2 mg/ml gelatin overnight to allow for adherence before NMD treatment. The cells treated with NMD were collected and washed once with PBS, then fixed with 4% paraformaldehyde for 30 min. After being washed twice with PBS, cells were incubated with the anti-cytochrome *c* (1:100; Cell Signaling) and anti-Bax antibodies (1:20; Cell Signaling) at 4°C overnight. The secondary antibodies fluorescein isothiocyanate-conjugated goat anti-mouse (Jackson immunoresearch, West Grove, USA) and phycoerythrin-conjugated anti-rabbit antibodies (Jackson immunoresearch) were used at 1:100 dilution at 4°C for 1 h. The cells were then incubated in 50 μg/ml DAPI solution (containing 100 μg/ml RNaseA) for 5 min at room temperature in the dark. After three times wash with PBS, the cells were observed using a fluorescence microscope (Zeiss).

Detection of autophagy by immunofluorescent staining

To detect the induction of autophagy morphologically in NMD-treated cells, HeLa cells (1×10^6) were treated with NMD at a final concentration of 10 μM for 6 and 12 h. Staining procedures were performed as previously described [18], and LC-3 antibodies were used to test the autophagy level of the cells. Images of LC-3 distribution in cells were captured using a Leica SP laser scan microscope system (Leica, Heidelberg, Germany). And cell structural alteration was examined by a transmission electron microscope (TEM; JEM2100HC, JEOL, Tokyo, Japan) [19].

Cloning, expression, and purification of Hsp90

The full-length Hsp90α and N-terminal Hsp90 (1–236AA) (N-Hsp90) were inserted into the expression vector pET28a, and transfected into the bacteria host BL21. Then, the bacteria were

cultured in LB medium in a 37°C incubator shaker at 250 rpm for 12 h, followed by IPTG induction accompanied with culture parameter adjustments including temperature shifted to16°C and shaking speed slowed down to 120 rpm for an additional 24 h cultivation. His tagged Hsp90 was purified with Ni-beads (GE healthcare, Bethesda, USA). All the procedures and methods had been described previously [14]. All Hsp90 and N-Hsp90 mentioned in this article were Hsp90 α.

Analysis of the interaction between Hsp90 and NMD

Fluorescent measurements and the ForteBio Octet Red system were used to analyze the interaction between N-Hsp90 and NMD.

Fluorescence intensities were recorded in the range of 290–500 nm at 293, 303, and 310 K, respectively, using a Cary Eclipse (Varian, Salt Lake City, USA). The experiments were performed in 2.0 ml of 5.0 μM N-Hsp90 solution (10 mM PBS buffer, pH 7.6) with successive additions of NMD solution (in 0.2% dimethyl sulfoxide, DMSO) from 0.5 to 50.0 μM. All tests were repeated in triplicate.

The interaction between Hsp90 and NMD was tested with the ForteBio Octet Red System (ForteBio, Inc., Menlo Park, USA). The biotinylated protein targets (e.g. Hsp90) were immobilized onto Super Streptavidin Biosensors, and the association and dissociation of the molecule NMD was monitored in parallel to save time. The light shift distance (nm) corresponding to association/dissociation time (in second). The dissociation constant K_D of NMD is calculated from the association and dissociation curve of NMD binding with Hsp90.

MDC staining

HeLa cells (1×10^6) were cultured with NMD for different time durations. The cells were harvested at the end of each treatment and stained with 50 μM MDC (diluted in PBS) at room temperature for 30 min in the dark. Then, the samples were washed with PBS twice and spun down at 106 *g* for 5 min to remove supernatant. The cells were then mounted on a glass slide for fluorescent detection with a Leica SP laser scan microscope system (Leica).

Data analysis

All data are presented as mean ± standard deviation and analyzed using Student's *t*-test. A *P*-value of <0.05 was considered statistically significant.

Results

NMD interacts with Hsp90

We investigated whether NMD could bind to Hsp90 and regulate its activity as an inhibitor of Hsp90. The binding of NMD with N-Hsp90 and full-length Hsp90 was characterized by the experiment of fluorescence measurements and the ForteBio Octet Red system. It was found that N-Hsp90 displayed maximal intrinsic fluorescence at 338 nm. When N-Hsp90 was incubated with NMD, the fluorescence intensity gradually decreased with increased concentrations of NMD (**Fig. 1A**). In the ForteBio Octet Red system, the binding of NMD to Hsp90 exhibited an association curve (**Fig. 1B**). The two dissociation

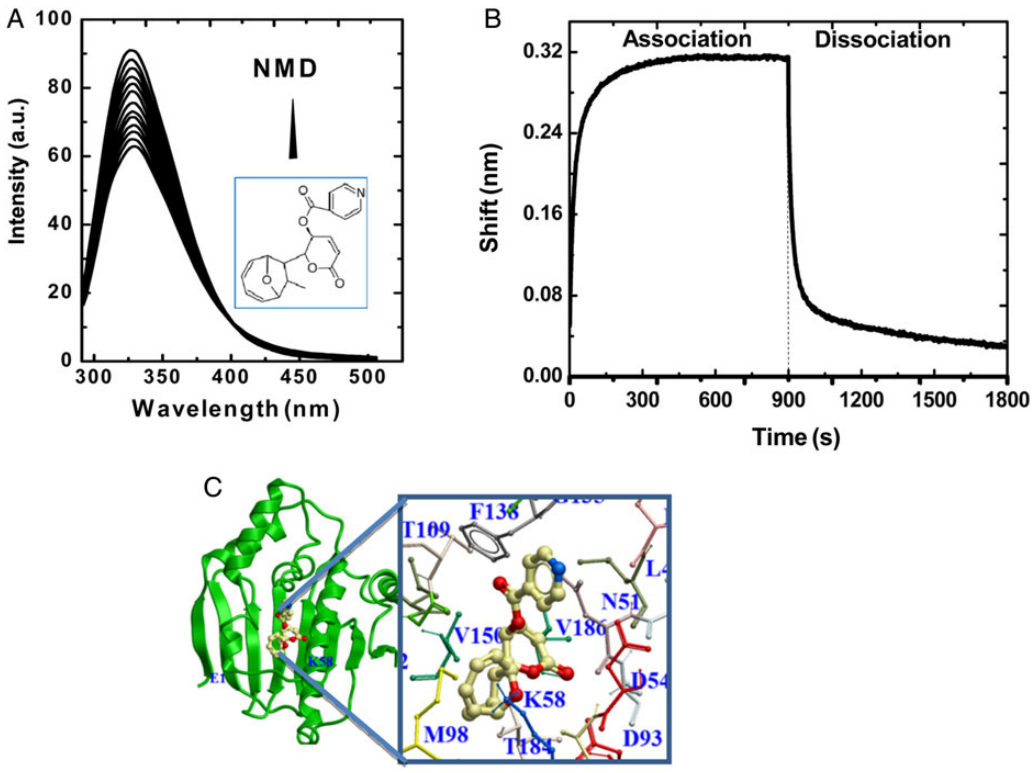

Figure 1. Hsp90 interacts with NMD (A) The vertical axis and horizontal axis represent the fluorescence intensity and emission wavelength, respectively. The excitation wavelength is 280 nm, whereas the emission peak for N-Hsp90 is 338 nm. The ratio of N-Hsp90 and NMD concentrations changed from 1:1 to 1:10. (B) The vertical axis and horizontal axis represent the light shift distance (nm) and association/dissociation time (s), respectively. The dissociation constant K_D of NMD is calculated from the association and dissociation curve of NMD with Hsp90. (C) Ribbon structure of N-Hsp90 with a ball-and-stick structure of NMD. Water molecules were not included in docking. The carbon and oxygen atoms of compound are yellow and red, respectively. The molecular docking model shows that NMD binds to ATP binding pocket of N-Hsp90. The main interaction is at the residues K58, T184 of Hsp90, and the NMD molecule.

constants (K_D) were 11.5 and 8 μM, calculated from the fluorescent spectrum and association/dissociation curve, which indicated that NMD bound to Hsp90 with a high affinity. The internal coordinate mechanics software was used to simulate the docking program of NMD with Hsp90. The crystal structure of full-length Hsp90 is from the protein data bank (PDB) (http://www.rcsb.org/pdb/home/home.do) with ID: 2CG9 (data not shown). Molecular docking result showed that NMD is in favor of binding Hsp90 at the N-terminus (PDB ID: 2CCS). The hydrogen bonds among the residues K58, T184, and NMD contributed to the main interaction (**Fig. 1C**). Hydrogen bond and van der Waals' force could be the main interaction factors between Hsp90 and NMD owing to a negative enthalpy change (-63.69 kJ mol^{-1}) and entropy change (-120.26 J mol^{-1} K^{-1}), which also supported the molecular docking result.

NMD degrades client protein Akt and triggers cytochrome *c* release

To illustrate the mechanism of NMD action on Hsp90, we further measured the expression levels of Hsp90 at NMD-treated HeLa cells by western blot analysis. After HeLa cells were treated for 24 h with 5, 10, or 15 μM NMD, the expression levels of Hsp90 were not changed, while the expression levels of Hsp70 were up-regulated and Akt expressions decreased significantly (**Fig. 2A**). The decreased expression levels of Akt were also observed in other tumor cell lines including HL-60, MDA-MB-231, AML21, and U2Os (**Fig. 2B**). Furthermore, immunofluorescent staining and western blotting were used to analyze pro-apoptotic proteins in cytosolic fractions. The results demonstrated that NMD exposure caused Bax to locate in the mitochondrion membrane (**Fig. 2C**), which led to cytochrome *c* (Cyt *c*) release from the mitochondria and increased cytosolic staining of Cyt *c* in HeLa cells (**Fig. 2D,E**).

NMD induces mitochondria apoptotic signaling in HeLa cells

To explore whether NMD-induced Cyt *c* release was correlated with mitochondrial dysfunction [20], we applied both fluorescence microscopy and flow cytometry to evaluate the mitochondrial membrane potential (MMP) change by probing MMP with the sensitive dye JC-1. It was found that the color of JC-1 staining changed from orange to green in HeLa cells after NMD treatment (**Fig. 3A**), indicating the loss of MMP, but the control cells exhibited orange or red colors. These results demonstrated that the MMP of HeLa cells were attenuated by treatment with NMD, owing to the Bax re-location in mitochondrial membrane (**Fig. 2C**).

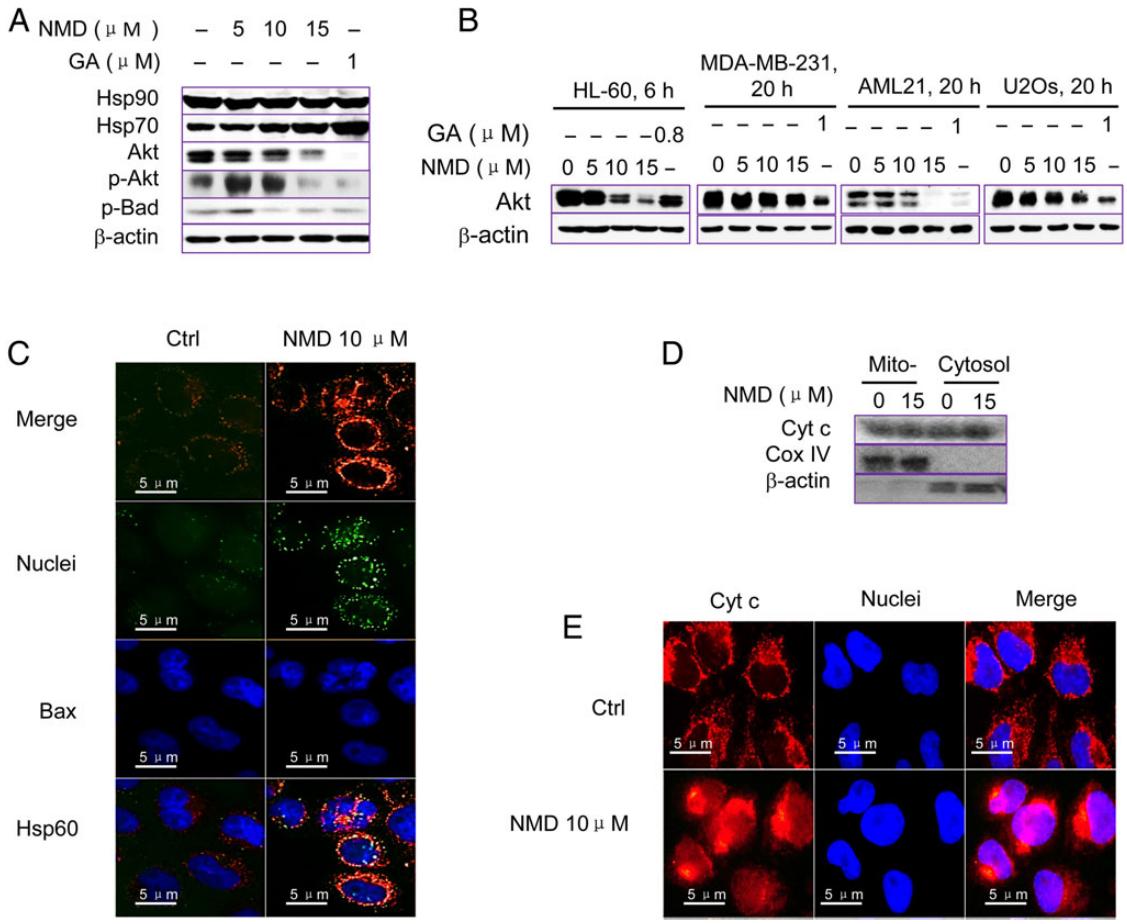

Figure 2. Hsp90 client protein degradation and Cyt *c* release in NMD-treated HeLa cells (A) HeLa cells were treated with NMD for 24 h at various concentrations. NMD-induced degradation of Akt, p-Akt, p-Bad, and Hsp70 were detected by western blot analysis using the specific antibodies. GA served as the positive control, and β-actin was used as a loading control. (B) NMD degraded Akt in other four tumor cells (HL-60, MDA-MB-231, AML21, and U2Os) was presented. (C) HeLa cells were treated with NMD for 20 h, and immunofluorescence assay was performed to monitor Bax localization (×50–65 folds). (D and E) HeLa cells were treated with 15 μM or 10 μM NMD for 24 h, and Cyt *c* release from mitochondria was assessed by (D) western blot analysis and (E) immunofluorescence analysis.

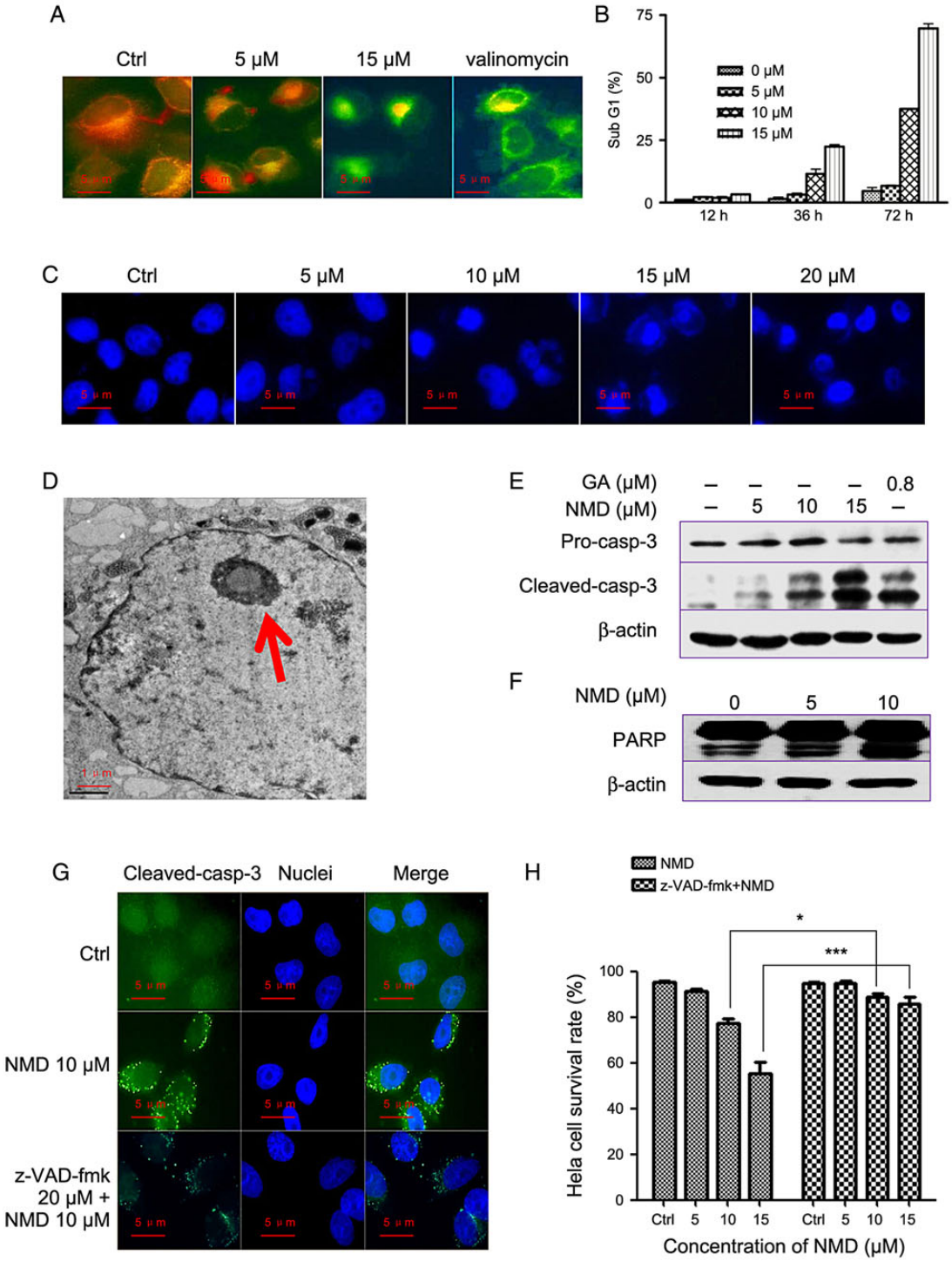

Figure 3. NMD induces mitochondria apoptosis in HeLa cells (A) HeLa cells were treated with vehicle control (DMSO), different concentrations of NMD or valinomycin (positive control) for 24 h before staining with JC-1 and analyzed by fluorescence microscopy. Scale bar is 5 μm. (B) HeLa cells treated with NMD for 12, 36, and 72 h at various concentrations were stained with PI. The distributions of the cell cycle stages were quantified by flow cytometry. (C) HeLa cells treated with different concentrations of NMD for 24 h were stained with DAPI or vehicle control. Scale bar is 5 μm. (D) HeLa cells were treated with NMD for 12 h. The figure showed the TEM view of the nuclei and chromosome condensation (red arrow). Scale bar is 1 μm. (E and F) HeLa cells were treated for 12 h with 5, 10 and 15 μM NMD, the pro-caspase-3 (~32 kDa) and PARP (~113 kDa) cleavage were assessed by western blot analysis. β-Actin was used as a loading control. (G) HeLa cells were treated with NMD (10 μM) and z-VAD-fmk for 12 h. Scale bar is 5 μm. (H) HeLa cells were pre-treated for 1 h with 20 μM caspase inhibitor, z-VAD-fmk and NMD, respectively, for 16 h, all groups were stained with PI. The level of relative cell survival (PI negative cells) was quantified by flow cytometry.

Besides the MMP dissipation and the release of Cyt *c*, NMD significantly influenced the cell cycle distribution of HeLa cells. About 25% cells were in the sub-G1 (sub-diploid apoptotic peak) phase after NMD treatment for 36 h. The sub-G1 phase was increased up to 75% within 72 h of exposure to NMD (**Fig. 3B**), and the cells underwent dramatic morphological changes, including nuclear envelope breakdown (**Fig. 3C**) and chromosome condensation (**Fig. 3D**). The observed morphological changes are consistent with those observed in apoptotic cells.

We investigated the additional mechanisms of apoptosis involved in NMD-induced cell death. In NMD-treated HeLa cells, both pro-caspase-3 (~32 kDa) and nuclear enzyme PARP (93 kDa) were cleaved into two fragments, respectively (**Fig. 3E,F**). The bands of 17 and 15 kDa were corresponding to cleaved caspase-3 (**Fig. 3E**); the bands of 89 and 34 kDa were corresponding to 113 kDa of PARP (**Fig. 3F**). The cleavage of pro-caspase-3 appeared in a bright green condensed form. Pre-treatment with z-VAD-fmk blocked the cleavage of pro-caspase-3 (**Fig. 3G**) and rescued the cell death (**Fig. 3H**), which suggested that NMD-induced apoptosis was caspase-dependent [21,22].

NMD suppresses cell survival and initiates cell autophagy

In NMD-treated cells, LC-3, which participates in the autophagy pathway, was activated after 6 h of treatment, and lasted for 24 h since the treatment beginning (**Fig. 4A**). The results from immunofluorescent staining further illustrated that LC-3 activation was initiated at 6 h after NMD treatment (**Fig. 4B**).

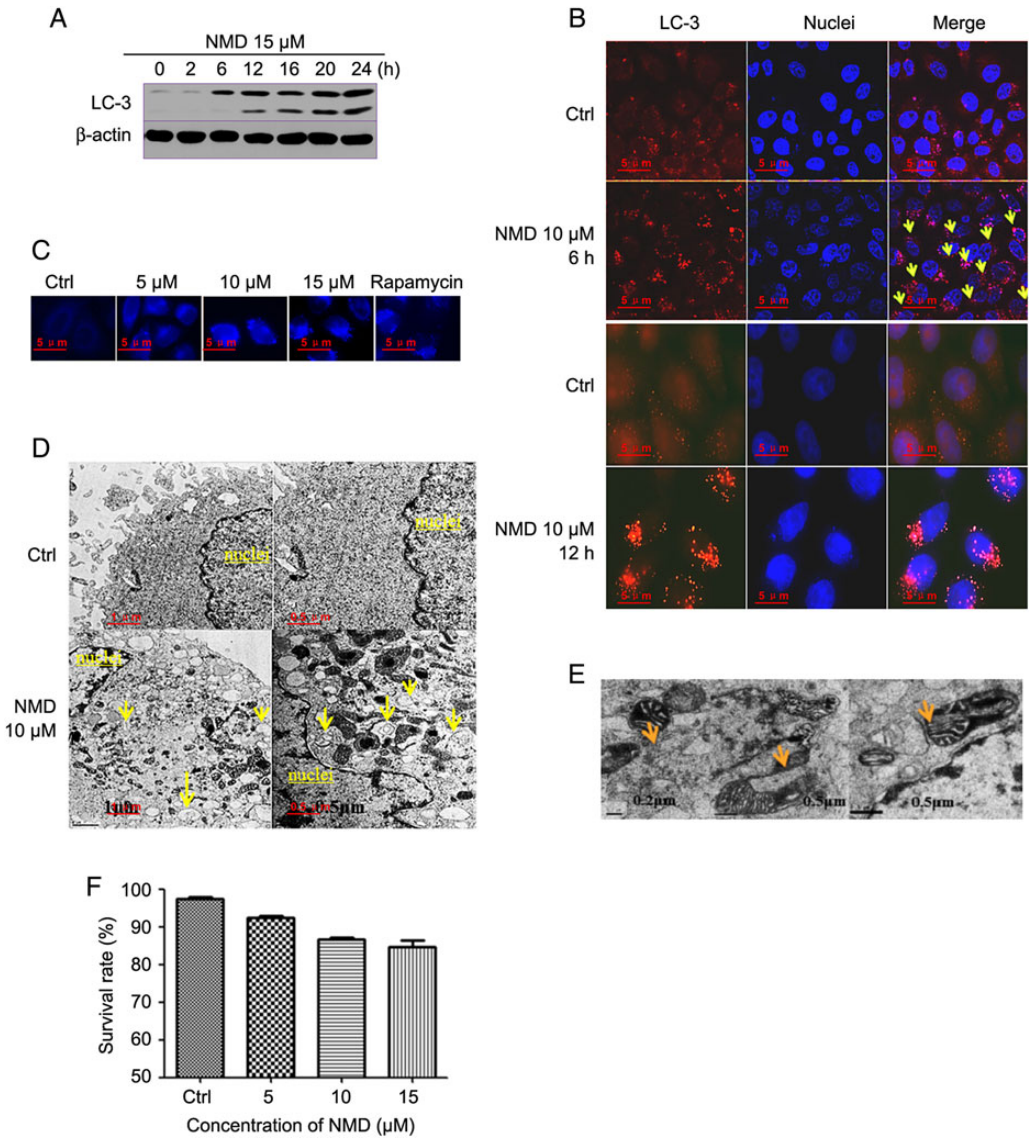

Figure 4. NMD regulates cell fates of HeLa cells (A) HeLa cells were treated for the indicated times with 15 μM NMD. Expression level of LC-3I/II in the presence of proteasome and autophagy inhibitors was assessed by western blotting. β-Actin was used as a loading control. (B) HeLa cells were treated for the indicated time with 10 μM NMD. The expression level of LC-3 was detected by immunofluorescence staining. NMD increased the expression level of LC-3, which appears as bright red dots, in both laser scanning confocal microscopy (top panel, 6 h) and fluorescent microscopy (bottom panel, 12 h). LC-3 is red and nuclei are blue. (C) MDC staining of autophagic vesicles. HeLa cells were treated with NMD for 12 h. (D and E) TEM view of the (D) autophagosome (yellow arrows) and (E) mitochondrial autophagosome (orange arrows). (F) HeLa cells treated with various concentrations of NMD for 24 h were stained with PI, and the level of relative cell survival (PI negative cells) was quantified by flow cytometry.

To confirm this result, we performed MDC staining and TEM to monitor the autophagic vacuoles. MDC is an acidotropic dye that stains late stage autophagosomes or autophagic vesicles. After HeLa cells were treated with NMD for 12 h, both MDC staining (**Fig. 4C**) and TEM imaging (**Fig. 4D**) showed the presence of autophagic vacuoles. Interestingly, TEM identified a population of mitochondria that exhibited autophagic vacuoles (**Fig. 4E**). These results suggest that NMD acts on Hsp90 and induces HeLa cell autophagy including dysfunctional mitochondria. We further explored whether NMD-induced autophagy caused cell death or suppressed cell survival. From the result of PI staining, we confirmed that NMD suppressed HeLa cell survival after 24 h of treatment (**Fig. 4F**).

NMD-induced autophagy is sensitive to chloroquine in HeLa cells

To illustrate the mechanism of NMD-induced autophagy, the expression levels of lysosomal-associated membrane protein 1 (LAMP1) and autophagy-related genes (BECN1) were analyzed in NMD-treated HeLa cells. The BECN1 expression is not sensitive to NMD treatment, while the expression of LAMP1 was significantly increased in NMD-treated HeLa cells (**Fig. 5A**). Furthermore, autophagy inhibitors (chloroquine, bafinomycin A1, and 3-MA) were added into NMD-treated HeLa cells. The results showed that NMD-induced autophagy is sensitive to chloroquine inhibition, but the other autophagy inhibitors including the bafinomycin A1 and 3-MA were less effective (**Fig. 5B,C**). We further found that both rapamycin and NMD-induced autophagy could be inhibited by chloroquine (**Fig. 5D**). From these results, we deduced that NMD-induced autophagy was in a lysosome-dependent manner.

Discussion

We demonstrated for the first time that the Hsp90 inhibitor NMD initiated the client protein degradation associated apoptosis and autophagy in HeLa cells. Hsp90 chaperones many client proteins, which play key roles in cell survival signaling pathway and many of them are onco-proteins. Apoptosis induced by NMD was associated with the degradation of Akt, one of Hsp90 client proteins. Akt signaling inactivates several pro-apoptotic factors, including Bad and other survival-related transcription factors. Akt phosphorylates Bad both *in vitro* and *in vivo*, and Akt-mediated Bad phosphorylation effectively blocks Bad-induced cell death [23,24]. In this study, we found that the degradation of Akt was associated with the decreased levels of its phosphorylated form, which might result in the decreased level of Bad phosphorylation. The activation of Bad is directly correlated with the re-location of pro-apoptotic protein Bax in mitochondria membrane which was followed by the loss of MMP and Cyt *c* release. All of these events finally contributed to the initiation of mitochondrial-dependent apoptosis.

We also showed that the novel compound NMD-induced apoptosis through mitochondrial disruption, which was different from the lead compound MED [25]. Hsp90-mediated NMD regulation on cell survival and apoptosis could be mediated by the degradation of the client protein Akt. Our results suggested that this novel compound was valuable for pharmaceutical industry as an anti-cancer drug candidate and a useful tool for further scientific research.

Cancer cell survival and apoptosis were believed to involve different signaling cascades, and most researches focused on cancer cell death pathways and mechanisms [7,26]. However, few studies concentrated on the transition state between survival and apoptosis. In this study, we found that autophagy mediated the transition between the cell survival and apoptotic signaling cascades in NMD-treated HeLa cells. Six hours after NMD treatment, there was no change in cell viability and the cell population in the sub-G1 phase was undetectable (**Fig. 3B**). However, HeLa cells at this point exhibited typical morphology of autophagy (**Fig. 3**), which was consistent with the results of Vucicevic *et al.* [27]. The Bax re-location in the mitochondria initiated Cyt *c* release, and subsequently induced cell apoptosis. The disruption of the MMP also activated lysosome-dependent autophagy to degrade the collapsed mitochondria.

During apoptosis, condensed chromosomes appeared after the occurrence of autophagosomes, which suggested that mitochondria with

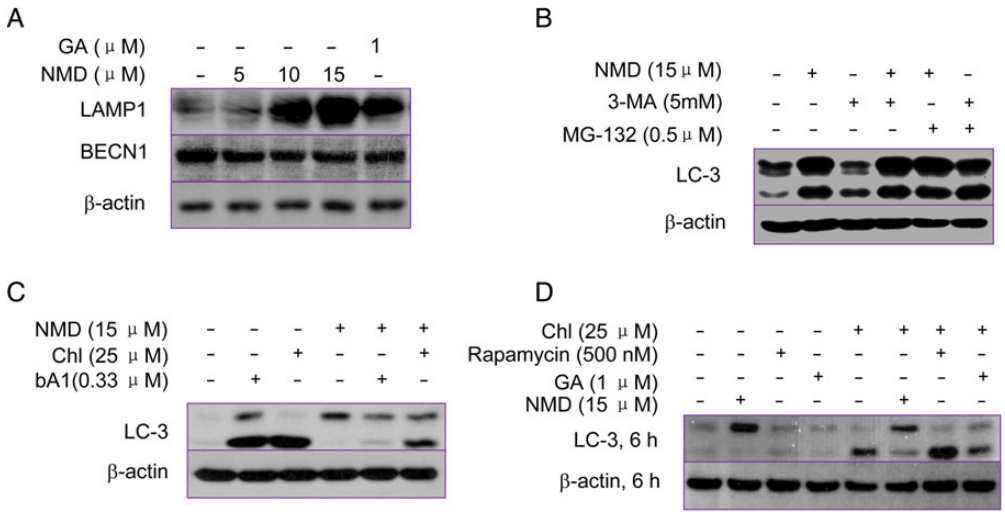

Figure 5. NMD-induced autophagy is sensitive to chloroquine in HeLa cells (A) HeLa cells were treated with NMD, after 16 h culture, the expression levels of LAMP1 and BECN1 were measured by western blotting. GA was used as a positive control. (B) HeLa cells were treated with NMD and 3-MA, separately or together for 16 h, the expression level of LC-3 was measured by western blotting. Proteosome inhibitor MG-132 was used as a control. (C) HeLa cells were co-treated with NMD and the inhibitors of chloroquine (Chl) and bafilomycin A1 (bA1) for 16 h, the expression level of LC-3 was measured by western blotting. β-Actin was included as a loading control. (D) HeLa cells were co-treated with NMD and the inhibitors of chloroquine (Chl), the expression level of LC-3 was analyzed by western blotting, rapamycin was used as the positive control. β-Actin was included as a loading control.

membrane potential dissipation can induce both apoptosis and autophagy. Autophagy is not a cell fate controller, but it mediates the cell's transition from survival to apoptosis. We deduced that autophagy may provide energy or material that is essential for apoptosis execution, by 'burning up' the cell debris (dissipation of mitochondrial membrane). The transition state of cancer cell (from survival to death) is similar to a melting pot in which autophagy, proliferation suppression, and apoptosis initiation all occur under NMD treatment. The encouraging results obtained in our laboratory demonstrated that LO2, a normal human liver cell line, is less sensitive to the cytotoxicity of NMD than many tumor cell lines. After LO2 cells were treated with NMD for 24 or 48 h, the result of MTS or MTT showed a very similar survival rate with the control DMSO group (data not shown), which suggested that the NMD may have advantages in target selectivity. However, the safety of NMD needs to be evaluated before it can be developed into a drug candidate. Exploring the relationship between apoptosis and autophagy is beneficial in understanding the complicated cell proliferation and death events. Compared with other Hsp90 inhibitors that had potencies as anti-tumor drug in clinical trial [28], NMD may not be a good inhibitor, but it exhibits the mechanisms of apoptosis and autophagy at cellular level, which may provide a clue for further in depth research. NMD not only has a potential to be a novel anti-tumor pharmaceutical, but also exhibits a new mechanism in regulating cancer cell apoptosis and autophagy via inhibiting Hsp90.

Funding

This work was supported by the grants from the National Natural Science Foundation of China (Nos. 81373296 and 30973566) and the Natural Science Foundation of Fujian Province of China (No. 2010J01227).

References

1. Roe SM, Prodromou C, O'Brien R, Ladbury JE, Piper PW, Pearl LH. Structural basis for inhibition of the Hsp90 molecular chaperone by the antitumor antibiotics radicicol and geldanamycin. *J Med Chem* 1999, 42: 260–266.
2. Whitesell L, Lindquist SL. HSP90 and the chaperoning of cancer. *Nat Rev Cancer* 2005, 5: 761–772.
3. Sreedhar AS, Soti C, Csermely P. Inhibition of Hsp90: a new strategy for inhibiting protein kinases. *BBA-Proteins Proteom* 2004, 1697: 233–242.
4. Taiyab A, Sreedhar AS, Rao CM. Hsp90 inhibitors, GA and 17AAG, lead to ER stress-induced apoptosis in rat histiocytoma. *Biochem Pharmacol* 2009, 78: 142–152.
5. Neckers L, Mollapour M, Tsutsumi S. The complex dance of the molecular chaperone Hsp90. *Trends Biochem Sci* 2009, 34: 223–226.
6. Eccles SA, Massey A, Raynaud FI, Sharp SY, Box G, Valenti M, Patterson L, *et al*. NVP-AUY922: a novel heat shock protein 90 inhibitor active against xenograft tumor growth, angiogenesis, and metastasis. *Cancer Res* 2008, 68: 2850–2860.
7. Jensen MR, Schoepfer J, Radimerski T, Massey A, Guy CT, Brueggen J, Quadt C, *et al*. NVP-AUY922: a small molecule HSP90 inhibitor with potent antitumor activity in preclinical breast cancer models. *Breast Cancer Res* 2008, 10: R33.
8. Lin TY, Bear M, Du Z, Foley KP, Ying W, Barsoum J, London C. The novel HSP90 inhibitor STA-9090 exhibits activity against Kit-dependent and -independent malignant mast cell tumors. *Exp Hematol* 2008, 36: 1266–1277.
9. Len N. Hsp90 inhibitors as novel cancer chemotherapeutic agents. *Trends Mol Med* 2002, 8: S55–S61.
10. Lin X, Huang YJ, Fang MJ, Wang JF, Zheng ZH, Su WJ. Cytotoxic and antimicrobial metabolites from marine lignicolous fungi, Diaporthe sp. *FEMS Microbiol Lett* 2005, 251: 53–58.
11. Stebbins CE, Russo AA, Schneider C, Rosen N, Hartl FU, Pavletich NP. Crystal structure of an Hsp90–geldanamycin complex: targeting of a protein chaperone by an antitumor agent. *Cell* 1997, 89: 239–250.
12. Li Y, Zhang T, Schwartz SJ, Sun D. New developments in Hsp90 inhibitors as anti-cancer therapeutics: mechanisms, clinical perspective and more potential. *Drug Resist Update* 2009, 12: 17–27.
13. Schulte TW, Neckers LM. The benzoquinone ansamycin 17-allylamino-17-demethoxygeldanamycin binds to HSP90 and shares important biologic activities with geldanamycin. *Cancer Chemoth Pharm* 1998, 42: 273–279.
14. Zhang L, Yi Y, Chen J, Zhang W, Huang Y, Zheng Z, Song S, *et al*. Probing target and designing nicotinoid derivatives for antiumor leading compoubd MED. *Chem J Chin Univ* 2010, 31: 1184–1189.
15. Shen YM, Zhang W, Zhang LR, Yi YT, Huang YJ, Zheng ZH, Song SY, *et al*. Synthesis and usage of 4-NDM, a nicotinic derivate of mycoepoxydiene. China Patent ZL201010150471.2.
16. Li Z, Jo J, Jia JM, Lo SC, Whitcomb DJ, Jiao S, Cho K, *et al*. Caspase-3 activation via mitochondria is required for long-term depression and AMPA receptor internalization. *Cell* 2010, 141: 859–871.
17. Zhang YB, Ye YP, Wu XD, Sun HX. Astilbotriterpenic acid induces growth arrest and apoptosis in HeLa cells through mitochondria-related pathways and reactive oxygen species (ROS) production. *Chem Biodivers* 2009, 6: 218–230.
18. Liu JJ, Zeng HN, Zhang LR, Zhan YY, Chen Y, Wang Y, Wang J, *et al*. A unique pharmacophore for activation of the nuclear orphan receptor Nur77 *in vivo* and *in vitro*. *Cancer Res* 2010, 70: 3628–3637.
19. Newman RA, Kondo Y, Yokoyama T, Dixon S, Cartwright C, Chan D, Johansen M, *et al*. Autophagic cell death of human pancreatic tumor cells mediated by oleandrin, a lipid-soluble cardiac glycoside. *Integr Cancer Ther* 2007, 6: 354–364.
20. Skommer J, Das SC, Nair A, Brittain T, Raychaudhuri S. Nonlinear regulation of commitment to apoptosis by simultaneous inhibition of Bcl-2 and XIAP in leukemia and lymphoma cells. *Apoptosis* 2011, 16: 619–626.
21. Xu M, Takanashi M, Oikawa K, Tanaka M, Nishi H, Isaka K, Kudo M, *et al*. USP15 plays an essential role for caspase-3 activation during Paclitaxel-induced apoptosis. *Biochem Biophys Res Commun* 2009, 388: 366–371.
22. Kothakota S. Caspase-3-generated fragment of gelsolin: effector of morphological change in apoptosis. *Science* 1997, 278: 294–298.
23. Datta SR, Dudek H, Tao X, Masters S, Fu H, Gotoh Y, Greenberg ME. Akt phosphorylation of BAD couples survival signals to the cell-intrinsic death machinery. *Cell* 1997, 91: 231–241.
24. Hennessy BT, Smith DL, Ram PT, Lu Y, Mills GB. Exploiting the PI3K/AKT pathway for cancer drug discovery. *Nat Rev Drug Discov* 2005, 4: 988–1004.
25. Wang JF, Zhao BB, Zhang W, Wu X, Wang RY, Huang YJ, Chen D, *et al*. Mycoepoxydiene, a fungal polyketide, induces cell cycle arrest at the G2/M phase and apoptosis in HeLa cells. *Bioorg Med Chem Lett* 2010, 20: 7054–7058.
26. Lauber K, Bohn E, Kröber SM, Xiao YJ, Blumenthal SG, Lindemann RK, Marini P, *et al*. Apoptotic cells induce migration of phagocytes via caspase-3-mediated release of a lipid attraction signal. *Cell* 2003, 113: 717–730.
27. Vucicevic L, Misirkic M, Kristina J, Vilimanovich U, Sudar E, Isenovic E, Prica M, *et al*. Compound C induces protective autophagy in cancer cells through AMPK inhibition-independent blockade of Akt/mTOR pathway. *Autophagy* 2011, 7: 40–50.
28. Kuhn DJ, Zeger EL, Orlowski RZ. Proteasome inhibitors and modulators of heat shock protein function. *Update Cancer Ther* 2006, 1: 91–116.